DOI: 10.61782/fa.2023.0449

forum acusticum 2023

IMPACT OF THE PHYSICAL PARAMETERS DESCRIBING THE RIGID POROUS MATERIALS ON THE REFLECTED LOW-FREQUENCY ULTRASONIC WAVE AT OBLIQUE INCIDENCE

Abdelmadjid Mahiou[1,2] **Mustapha Sadouki**[1*]
[1] Acoustics and Civil Engineering Laboratory, Khemis-Miliana University, Algeria
[2] Theoretical Physics and Radiation Matter Interaction Laboratory, Soumaa, Blida, Algeria

ABSTRACT

Several studies have been carried out showing the effect of the physical parameters describing the porous medium on the transmitted or reflected signals at normal incidence [Proc. Mtgs. Acoust. 45, 045004 (2021)]. In this work, a numerical simulation study is proposed to highlight the effect of some physical parameters on the reflected signal in oblique incidence in the context of the equivalent fluid theory. The objective of this work is to show the influence of these physical parameters on the reflected signal in a low-frequency ultrasound regime as a function of the angle of incidence. The measurements were made for an excitation frequency of 55 kHz at angles of incidence varying between 5° and 45°. The parameters studied are those involved in the corrected Johnson-Allard model recently introduced by Sadouki [Phys. Fluids 33, (2021)], namely; porosity tortuosity viscous and thermal characteristic lengths as well as both viscous and thermal shape factors. The results obtained are discussed and compared with those given in the literature.

Keywords: *Porous material, acoustic reflected waves, low frequency ultrasound, equivalent fluid theory.*

1. INTRODUCTION

Porous materials with rigid or flexible structures are commonly used in applications where acoustic performance is essential. The Johnson-Champoux-Allard (JCA) model [1-3] is a semi-phenomenological model that describes the acoustic behavior of an acoustic porous material with an immobile skeleton of any pore shape. To calculate the dynamic density of the material, the JCA model involves four parameters, including open porosity, static airflow resistivity, the high-frequency limit of tortuosity, and viscous characteristic length.

Similarly, the dynamic compressibility modulus of the material is determined using the open porosity and thermal characteristic length. The JCA model approximations have simple expressions for the high-frequency limit and the low-frequency limit of the imaginary part. The model was refined by introducing viscous and thermal form factors (ξ and ξ') to fit the ultrasonic low-frequency limit. These two form factors played a crucial role in stabilizing and improving the values of tortuosity, viscous, and thermal characteristic lengths in the transmitted signals [4].

Previous studies [5,6] have been conducted to demonstrate the impact of these parameters on normally transmitted and reflected signals in the low-frequency ultrasound regime. In this paper, we propose a numerical simulation method to investigate the effect of the fitted JCA model [1] refined by Sadouki parameters on the attenuation of obliquely incident reflected waves by an air-saturated rigid porous material in the low-frequency ultrasound regime. We performed measurements for an excitation frequency of 55 kHz at incidence angles ranging from 5 to 45 degrees. The purpose of the study is to rank these parameters according to their decreasing order of influence in oblique incidence reflection mode. The results of this study will aid in enhancing the acoustic performance of porous materials and provide insight into their practical applications.

2. MODEL

In the context of a rigid frame air-saturated porous medium subjected to acoustic excitation, any structural vibrations can be assumed negligible and, therefore, ignored. Consequently, the waves in this media propagate solely through the fluid. To investigate the

[*] ***Corresponding author***: mustapha.sadouki@univ-dbkm.dz

propagation of acoustic waves in such scenarios, the equivalent fluid theory is employed [1], which is a particular case of the Biot model[7]. This theory incorporates fluid-structure interactions by considering two frequency response factors: the dynamic tortuosity of the medium, α(ω), as formulated by Johnson et al [3], and the dynamic compressibility of air in the porous material, β(ω), as given by Allard [1,2]. These factors, in the frequency domain, are multiplied by the density and compressibility of the fluid. The high-frequency regime is determined when the viscous skin depth $\delta(\omega)$ is greater than the characteristic pore length r. ($\delta(\omega) = \sqrt{\frac{2\eta}{\rho_0 \omega}}$, where ρ_0 is the density of the saturating fluid, η is the viscosity, ω the pulsation frequency, P_r the Prandtl number). At low ultrasonic frequencies, the corrected dynamic tortuosity α(ω) and dynamic compressibility β(ω) are expressed as follows[4]:

$$\alpha_{\sim\delta^2}(\omega) = \alpha_\infty \left(1 + \frac{\delta(\omega)}{\Lambda}\left(\frac{2}{j}\right)^{\frac{1}{2}} + \xi\left(\frac{\delta(\omega)}{\Lambda}\right)^2\left(\frac{2}{j}\right) + \cdots\right), \quad (1)$$

$$\beta_{\sim\delta^2}(\omega) = 1 + (\gamma - 1)\left(\frac{\delta'(\omega)}{\Lambda'}\left(\frac{2}{j}\right)^{1/2} + (\xi' - 1)\left(\frac{\delta'(\omega)}{\Lambda'}\right)^2\left(\frac{2}{j}\right)\right) \quad (2)$$

Where, $j = \sqrt{-1}$ and γ is the adiabatic constant.
The models used for studying acoustic waves in porous media rely on several physical parameters. One such parameter is the high-frequency limit of the tortuosity of the medium, denoted by α_∞, which was first introduced by Zwikker and Kosten [8]. The viscous and thermal characteristic lengths Λ and Λ' were introduced by Johnson and Allard [1-3]. Another important parameter is the dimensionless factor ξ introduced by Sadouki [4], which characterizes the correction for the viscous skin depth in the low-frequency regime of ultrasonic waves near the tube surface. The velocity distribution near the surface is significantly disturbed by the viscous forces generated by the motionless frame, making ξ a relevant factor to consider. Additionally, there is an associated thermal counterpart to ξ, denoted by ξ'.

To further understand the behavior of acoustic waves in porous media, consider an isotropic and homogeneous porous medium that spans the region $0 \leq x \leq L$ (Fig.1).

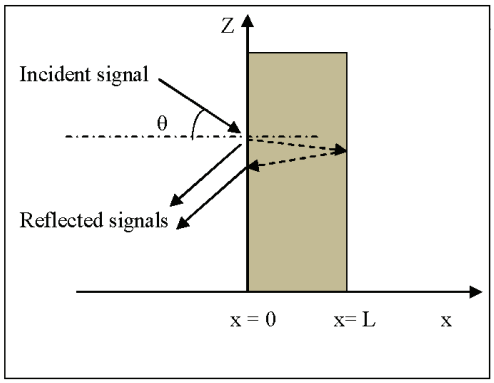

Figure 1. Problem geometry

When an acoustic wave with oblique incidence $\theta \neq 0$ reaches the first interface of the medium, it generates an acoustic pressure field $p(x,\omega)$ and an acoustic velocity field $v(x,\omega)$ within the material. These fields are governed by the Euler equation and the constitutive equation along the x-axis.

$$\begin{cases} \rho_0\, \alpha(\omega) j\omega\, v(x,\omega) = \frac{\partial p(x,\omega)}{\partial x} \\ \frac{1}{K_a}\beta(\omega) j\omega\, p(x,\omega) = \frac{\partial v(x,\omega)}{\partial x} \end{cases} \quad (3)$$

with $K_a$is the compressibility modulus of the saturating fluid. Applying the continuity conditions of the pressure and velocity fields at the boundary of the medium, we end up with the following reflection coefficient of the porous material:

$$R(\omega) = \frac{(1-E^2)sinh(s\,L\,f_1)}{(1+E^2)sinh(s\,L\,f_1)+2\,E\,cosh(s\,L\,f_1))} \quad (4)$$

where, $E = \phi\,\frac{cos\theta_1}{cos\theta_0}\sqrt{\frac{\beta(\omega)}{\alpha(\omega)}}$, $f_1 = cos\theta_1\sqrt{\frac{\rho_f}{K_a}\alpha(\omega)\beta(\omega)}$

and $cos\theta_1 = \sqrt{1 - \frac{sin\theta_0{}^2}{\alpha(\omega)\beta(\omega)}}$, ϕ is porosity.

The incident and the reflected fields p^i and p^r_{sim} are related in frequency domain by the reflection coefficient R:

$$p^r_{sim}(x,\omega) = R(\omega)\, p^i(x,\omega) \quad (5)$$

In the time domain, the simulated reflected signal $p_{sim}^{t}(x,t)$ is obtained numerically by taking the inverse Fourier transform $\mathcal{F}^{-1}$ of the previous equation,

$$p_{sim}^{t}(x,t) = \mathcal{F}^{-1}\left(R(\omega)\, p^{i}(x,\omega)\right) \qquad (6)$$

3. SIMULATED STUDY

The simulation study enabled us to generate the incident and reflected signals of a single-layer porous medium, constructed in the frequency and time domain using equations (5) and (6), respectively. In our study, the porous medium depicted in Fig.1 had the following characteristics: L = 2.0 cm, $\phi = 0.84$, $\alpha_{\infty} = 1.2$, $\Lambda = 230\,\mu m$, $\Lambda'/\Lambda = 2$, $\xi = 10$, and $\xi/\xi' = 3.0$. The signals were created with a center frequency peak of 55 kHz, and the results obtained from the simulation are presented in Figure 2. Both the time and frequency figures show clear amplitudes of the reflection at the first and second interfaces.

Next, we focus on the frequency regime study of the simulation, where incident waves are observed with angles of incidence varying from 5° to 45°, with a step of 10°.

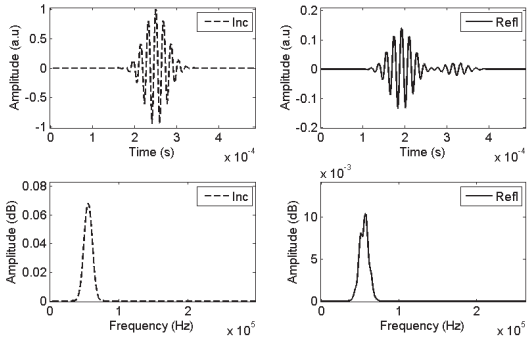

Figure 2. Simulated incident and reflected signals from a single-layer porous medium constructed in frequency domain using Eq. 5 and in time domain using Eq. 6, for an incidence angle of 5° and a central frequency of 55 kHz

3.1 Effect of the porosity ϕ on the reflected signal

Figure 3 illustrates the sensitivity of the reflected signal to variations in porosity at an excitation frequency of 55 kHz and two incidence angles ($\theta = 5°$ and $\theta = 45°$). The results demonstrate a significant sensitivity of the reflected signal to a ±20% variation in initial porosity. Specifically, at an incidence angle of 5°, a 20% increase in porosity results in a substantial 63.34% decrease in the modulus of the reflected signal, while a 20% decrease in porosity leads to a considerable 75.32% increase in the amplitude of the reflected signal. These findings indicate that porosity has a substantial impact on the reflected signal, and the relative change in the amplitude of the reflected signal is inversely proportional to porosity.

Furthermore, Table 1 highlights that the effect of porosity on the reflected signal varies with the angle of incidence. The sensitivity of porosity increases as the angle of incidence increases, emphasizing the importance of conducting a thorough analysis of the impact of porosity in single-layer porous media.

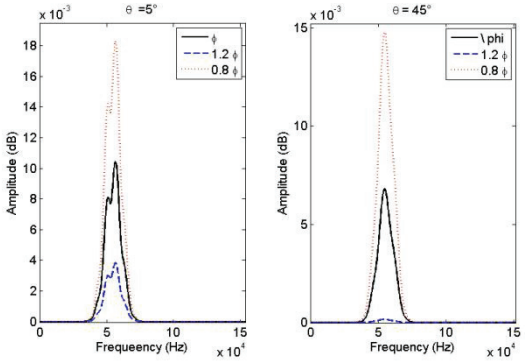

Figure 3. Effect of a ±20% variation in ϕ on the amplitude of the reflected wave at 55kHz for waves of 5° and 45° incidence

Table 1. - Relative variation of the reflected wave amplitude as a function of ϕ the angle of incidence at the frequency 55kHz.

		ϕ	
		+20%	-20%
$\frac{\Delta R}{R}\%$	$\theta_0 = 5$	-63.34%	75.32%
	$\theta_0 = 15$	-65.08%	77.71%
	$\theta_0 = 25^{\circ}$	-68.82%	82.07%
	$\theta_0 = 35^{\circ}$	-77.45%	92.69%
	$\theta_0 = 45°$	-97.51%	117.45%

3.2 Effect of the tortuosity α_∞ on the reflected signal

The sensitivity of the reflected signal to variations in tortuosity can be seen in Fig. 4. For an excitation frequency of 55 kHz and incidence angles of $\theta = 5°$ and $\theta = 45°$, the reflected signal exhibits significant sensitivity to a ±20% variation in initial tortuosity. Specifically, a +20% increase in tortuosity results in a 24.74% increase in the modulus of the reflected signal, while a -20% decrease in tortuosity results in a -33.31% decrease in the amplitude of the reflected signal for an angular incidence of 5°. These results clearly indicate that tortuosity has a substantial impact on the reflected signal. Furthermore, it should be noted that the influence of tortuosity on the reflected signal varies with the angle of incidence, as shown in Tab. 2. The data reveal that the sensitivity of tortuosity decreases for an incidence angle of 45°, which highlights the importance of a thorough examination of the impact of tortuosity and porosity on reflected signals in single-layer porous media.

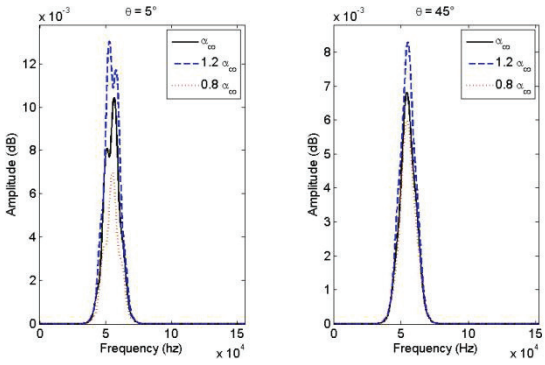

Figure 4. Effect of a ±20% variation in $\boldsymbol{\alpha_\infty}$ on the amplitude of the reflected wave at 55kHz for waves of 5° and 45° incidence

Table 2 - Relative variation of the reflected wave amplitude as a function of $\boldsymbol{\alpha_\infty}$ and the angle of incidence at the frequency 55kHz.

		α_∞	
		+20%	-20%
$\frac{\Delta R}{R}\%$	$\theta_0 = 5$	24.74%	-33.31%
	$\theta_0 = 15$	42.69%	-29.68%
	$\theta_0 = 25^\circ$	30.00%	-38.43%
	$\theta_0 = 35^\circ$	15.05%	-25.30%
	$\theta_0 = 45°$	21.84%	-12.04%

3.3 Effect of viscous characteristic length $\boldsymbol{\Lambda}$ on the reflected signal

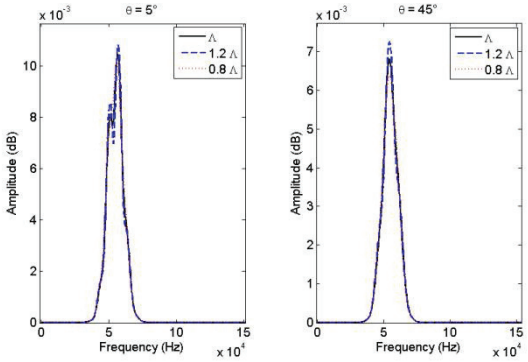

Figure 5. Effect of a ±20% variation in $\boldsymbol{\Lambda}$ on the amplitude of the reflected wave at 55kHz for waves of 5° and 45° incidence

Figure 4 shows the effect of varying the viscous characteristic length on the reflected signal at the low ultrasonic frequency. For an excitation frequency of 55 kHz and an incidence angle of $\theta = 5°$, a 3.57% change in the amplitude of the reflected signal was observed for a 20% increase in the initial value of the viscous characteristic length Λ. In addition, the amplitude of the reflected signal dereased slightly by -2.36% for a -20% change in the initial value of the relevant parameter. Thus, we conclude that the variation of the viscous characteristic length has a small effect on the reflected signal. This influence increases as the incidence angle increases, as shown in Tab.3.

Table 3 - Relative variation of the reflected wave amplitude as a function of Λ and the angle of incidence at the frequency 55kHz.

.

		$\Lambda\ (m)$	
		+20%	-20%
$\frac{\Delta R}{R}\%$	$\theta_0 = 5$	3.57%	-2.36%
	$\theta_0 = 15$	1.94%	-0.46%
	$\theta_0 = 25^\circ$	6.21%	-5.19%
	$\theta_0 = 35^\circ$	02.82%	-1.77%
	$\theta_0 = 45°$	6.66%	-6.05%

3.4 Effect of thermal characteristic length $\boldsymbol{\Lambda'}$ on the reflected signal

Figure 6 shows the effect of varying the thermal characteristic length Λ on the reflected signal at the low

frequency of ultrasound. For an excitation frequency of 55 kHz and incidence angles of 5° and 45°, a +20% and -20% variation in Λ results in a +0.62% and -0.91% variation in the amplitude of the reflected signal for the 5° incidence angle, and a relative variation of +1.38% and -2.02% in the amplitude for the 45° incidence angle, as presented in Tab4. Our conclusion is that the thermal characteristic length Λ has a minor impact on the reflected signal, which grows with the incidence angle.

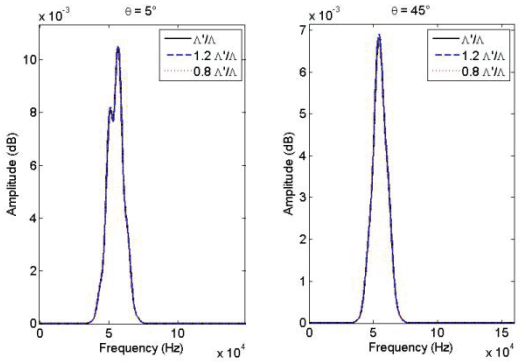

Figure 6. Effect of a ±20% variation in $\boldsymbol{\Lambda'}$ on the amplitude of the reflected wave at 55kHz for waves of 5° and 45° incidence

Table 4 - Relative variation of the reflected wave amplitude as a function of Λ and the angle of incidence at the frequency 55kHz.

.

		$\Lambda'(m)$	
		+20%	-20%
$\frac{\Delta R}{R}\%$	$\theta_0 = 5$	0.62%	-0.91%
	$\theta_0 = 15$	0.43%	-0.56%
	$\theta_0 = 25^\circ$	1.09%	-1.61%
	$\theta_0 = 35^\circ$	0.66%	-1.04%
	$\theta_0 = 45°$	1.38%	-2.02%

3.5 Effect of viscous shape factor ξ on the reflected signal

The analysis of the curve shown in Figure 6 indicates that the impact of the viscous shape factor ξ on the amplitude of the reflected wave is very small. At an excitation frequency of 55 kHz and an incidence angle $\theta = 5°$, a ±20% variation in ξ results in a maximum amplitude change of only -1.40% and +1.73%, which is negligible. Similarly, at an incidence angle of 45°, the maximum amplitude change due to a ±20% variation in ξ is only-1.22% and +1.86%, which is also very small. This is consistent with the data presented in Tab.5, which shows that the influence of ξ on the reflected signal is small and sometimes negligible.

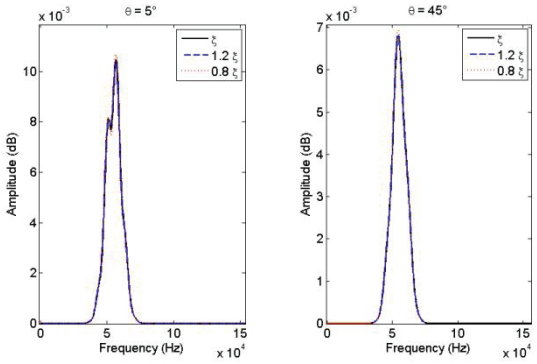

Figure 7. Effect of a ±20% variation in ξ on the amplitude of the reflected wave at 55kHz for waves of 5° and 45° incidence

Table 5 - Relative variation of the reflected wave amplitude as a function of ξ and the angle of incidence at the frequency 55kHz.

		ξ	
		+20%	-20%
$\frac{\Delta R}{R}\%$	$\theta_0 = 5$	-1.40%	1.73%
	$\theta_0 = 15$	-0.98%	1.43%
	$\theta_0 = 25^\circ$	-1.54%	1.92%
	$\theta_0 = 35^\circ$	-1.22%	1.48%
	$\theta_0 = 45°$	-1.55%	1.86%

3.6 Effect of the thermal shape factor ξ' on the reflected signal

Figure 8 displays the impact of the thermal shape factor ξ` on the low-frequency reflected ultrasound signal for incidence angles of 5° and 45°. The values recorded in Tab.6 indicate that this parameter has a negligible effect on the amplitude of the reflected signal. When the initial value of the thermal shape factor is changed by +20% or -20%, the modulus of the reflected signal experiences a slight increase of 0.07% or a decrease of -0.01%, respectively. This variation remains almost constant as the angle of incidence varies from 5° to 45°.

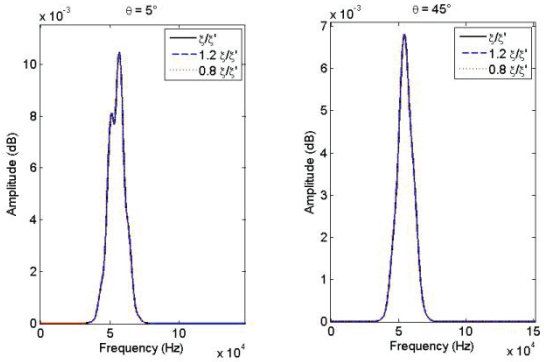

Figure 8. Effect of a ±20% variation in ξ' on the amplitude of the reflected wave at 55kHz for waves of 5° and 45° incidence

Table 6 - Relative variation of the reflected wave amplitude as a function of ξ' and the angle of incidence at the frequency 55kHz.

		ξ/ξ'	
		+20%	-20%
$\frac{\Delta R}{R}\%$	$\theta_0 = 5$	0.07%	-0.10%
	$\theta_0 = 15$	0.05%	-0.08%
	$\theta_0 = 25^\circ$	0.08%	-0.12%
	$\theta_0 = 35^\circ$	0.06%	-0.09%
	$\theta_0 = 45°$	0.07%	-0.10%

4. CONCLUSION

We conducted a sensitivity study on several physical parameters describing a single-layer porous material using low-frequency ultrasound. The study involved analyzing the impact of a ±20% variation in porosity (ϕ), tortuosity (α_∞), viscous and thermal characteristic length (Λ and Λ'), and viscous and thermal shape factors (ξ and ξ') on the amplitude of the obliquely reflected signal.

Our results indicate that porosity has a significant influence on the amplitude of the reflected signal in the low-frequency ultrasound regime, which increases with frequency and angle of incidence. We also found that tortuosity has a noticeable impact, while the influence of viscous characteristic length , thermal characteristic length, and the two shape factors ξ and ξ' is small and sometimes negligible on the amplitude of the reflected signal. However, we observed that the sensitivity of these parameters increases for an incidence angle of 45°. These results can be used in inverse problem solving, which involves determining the physical parameters of a porous medium by minimizing the difference between the experimental and simulated signals. It is important to note that the choice of frequency and angle of incidence of the ultrasonic wave is crucial for the accurate characterization of these media. Therefore, these criteria must be carefully selected to obtain good and optimal results.

4. ACKNOWLEDGMENTS

This work was supported by the General Directorate of Scientific Research and Technological Development (DGRSDT), Algeria, under the number B00L02UN44012020001 (PRFU).

5. REFERENCES

[1] J. F. Allard, "Propagation of sound in porous media," Elsevier Applied Science publishers LTD, 1993.

[2] D. Lafarge, P. Lemarinier, J. F. Allard, and V. Tarnow, "Dynamic compressibility of air in porous structures at audibles frequencies," J. Acoust. Soc. Am, vol. 102, no. 4, pp. 1995-1997, 1997.

[3] D. L. Johnson, T. J. Plona, C. Scala, F. Pasierb, and H. Kojima, "Tortuosity and acoustic slow waves," Phys. Rev. Lett., vol. 49, pp. 1840, 1982.

[4] M. Sadouki, "Experimental characterization of air-saturated porous material via low-frequencies ultrasonic transmitted waves," Physics of Fluids, vol. 33, no. 3, pp. 037102, 2021.

[5] A. Mahiou, I. Sellami, and M. Sadouki, "Sensitivity of transmitted low-frequency ultrasound physical parameters describing a rigid porous material," Proc. Mtgs. Acoust., vol. 45, pp. 045004, 2021.

[6] M. Sadouki, A. Mahiou, and N. Souna, "Effect of acoustic low-frequency ultrasound parameters on the reflected signal from a rigid porous medium," Proc. Mtgs. Acoust., vol. 50, no. 1, pp. 045002, 2022.

[7] M. A. Biot, "The theory of propagation of elastic waves in a fluid-saturated porous solid. higher frequency range," J. Acoust. Soc. Am., vol. 28, pp. 179, 1956.

[8] C. Zwikker and C. W. Kosten, "Sound absorbing materials," Elsevier, New York, 1949.